Pernicious effect of physical cutoffs in fractal analysis

M. Ciccotti* and F. Mulargia

Settore di Geofisica, Dipartimento di Fisica, Università di Bologna, Viale Berti Pichat, 8 Bologna, Italy

Fractal scaling appears ubiquitous, but the typical extension of the scaling range observed is just one to two decades. A recent study has shown that an apparent fractal scaling spanning a similar range can emerge from the randomness in dilute sets. We show that this occurs also in most kinds of nonfractal sets irrespective of defining the fractal dimension by box counting, minimal covering, the Minkowski sausage, Walker's ruler, or the correlation dimension. We trace this to the presence of physical cutoffs, which induce smooth changes in the scaling, and a bias over a couple of decades around some characteristic length. The latter affects also the practical measure of fractality of truly fractal objects. A defensive strategy against artifacts and bias consists in carefully identifying the cutoffs and a quick-and-dirty thumb rule requires to observe fractal scaling over at least three decades.

I. INTRODUCTION

The original definition of "fractal" is strictly related to the evaluation of the Hausdorff-Besicovitch dimension of a geometric set provided that this is not an integer. Since this definition is of difficult applicability, several alternative operational definitions are preferred, such as box counting, its mathematical twin the Minkowski sausage, and Walker's ruler.

The concept of "fractals" was then extended to include sets in which the number N of objects of diameter up to L scales as a power law with fractional exponent D. This definition disregards the location of the elements in the set and is not simply amenable to a geometric dimension. One more class of sets that has been included in the definition is the one in which the distribution of some more general property P (such as the earthquake magnitude) scales as a power law with the fractional exponent, which disposes of any link with the geometry.

Considering the distribution of higher-order moments, the generalized fractal dimension D_q is defined with D_0 the classical fractal dimension (capacity), D_1 being the information dimension and D_2 the correlation dimension. If these dimensions have different values, the set is called a "multifractal." The evaluation of the correlation dimension D_2 is the scope of the Grassberger and Procaccia algorithm, which is commonly used to study the time or space distribution of point events and the "strangeness" of the attractors of chaotic orbits.

Although fractality ideally implies a power-law relation over an infinite range of scales, it is measured only over a very limited interval in most practical cases. Fractal analysis must face not only the two obvious cutoffs related to the limited resolution and extension of the images or data sets, but also other physical cutoffs linked to the measurement procedure or to the presence of characteristic lengths. All these cutoffs will be shown to have a critical importance in defining the fractal nature of the system.

---

*Email address: matteo@ibogeo.df.unibo.it

II. PHYSICAL CUTOFFS AND THE DIMENSION OF EMPIRICAL SETS

The scope of this paper is limited to fractal analysis in relation to the geometric dimension, which considers sets of two main categories. The first one regards small unconnected objects, such as points, rods, spots, etc. Their fractal dimension (between 0 and the dimension of the embedding space) indicates clustering in their spatial distribution. Typical examples are earthquake epicentral maps, lake or mining resources maps, spatial distribution of pores or impurities, and time series. The second category regards connected sets and typical examples are topographic contours, piecewise linear patterns (such as geologic fault patterns), contour surfaces, or surface patterns in three-dimensional (3D) images, etc. The fractal dimensions of these categories are, respectively, greater than 1 and 2 and characterize the roughness and the branching complexity of the shapes.

The scaling behavior can be different over different ranges of scales. For example, a series of equispaced points on a line will scale with dimension zero at scales much smaller than the interpoint distance Δ, and with dimension 1 (linelike) for scales much larger than this. If the points are substituted with rods of length d, three different scaling laws appear, since the set has again dimension 1 for scales much smaller than d. However, for the dimension zero to be well defined in the intermediate region, the distance between the two cutoffs must be sufficiently large. A set of balls of radius R in a N-dimensional embedding space will always scale as N dimensional for scales much smaller than R; information about the spatial distribution of balls would only emerge at somewhat larger scales. Similarly, in a set of small fractals of extension R distributed in space following a different fractal distribution than their internal one, the fractal dimension of the objects will prevail for scales much smaller than R, while the fractal dimension of their spatial distribution will prevail for much larger ones. In general, stopping the generating process of a fractal set at some finite step in which the smallest details are segments of length d, dimension 1 would prevail. Contour lines and line networks always scale as one dimensional below the length of the smallest traced segment.
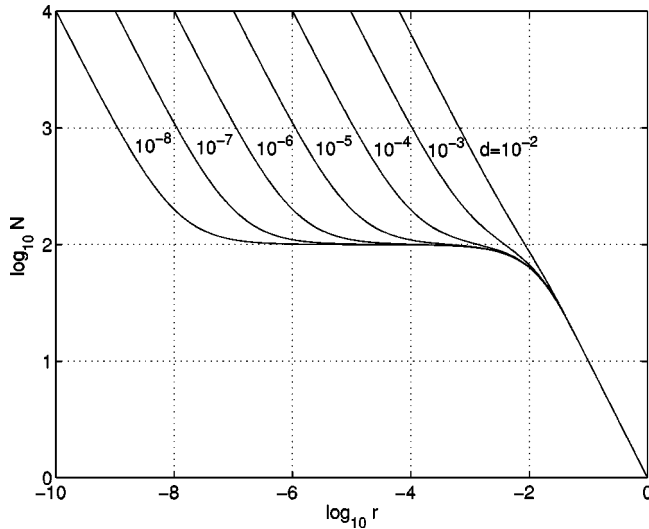
FIG. 1. Box counting $N(r)$ curves for random sets of $M = 100$ rods for several values of the radius d. All lengths are normalized to the unit side of the analyzed sets.

At the same time, extending the analysis below the width of the traced lines, dimension 2 will prevail, while measuring the scaling much beyond the extension of the object will give dimension zero since this will appear isolated.

III. FRACTAL ANALYSIS

A. Several capacity dimensions

Since the original *capacity* or *minimal covering* fractal dimension is cumbersome and time consuming in more than one dimension [1], alternative definitions, more computationally efficient, were proposed. One of the most popular of these definitions is the *box counting* (BC). The covering is obtained by considering a uniform partition (generally dyadic) made of nonoverlapping boxes of radius r, and then counting the number of boxes $N(r)$ that have a nonempty intersection with the set. Automatization of BC requires the digitization of the sets, and the fractal dimension D_{BC} is generally estimated through a least squares linear fit. Several traps are hidden in this apparently simple process, often leading to wrong dimension estimates [2,3].

A very similar method, called *Minkowski sausage* (MS), consists of taking a ball of radius r around each point of the set and evaluating the volume $V(r)$ of the union of all balls. A fractal dimension D_{MS} prevails at some range if the quantity $N(r) = V(r)/V_B(r)$ obeys a power law in that range (V_B is the volume of each ball).

Hamburger *et al.* [4] derived an analytical calculation of the expected scaling curves $N(r)$ for a set of randomly distributed balls analyzed by BC and MS methods. Typical BC curves of $N(r)$ and local fractal dimension for 1D balls are reported in Figs. 1 and 2 for several values of the diameter d of the balls. Examining these in terms of cutoffs, one sees that two of these are apparent, respectively, related to the diameter d and to the average free distance Δ. Dimension 1 prevails at scales external to these cutoffs, while dimension zero may only be established in the intermediate region if the
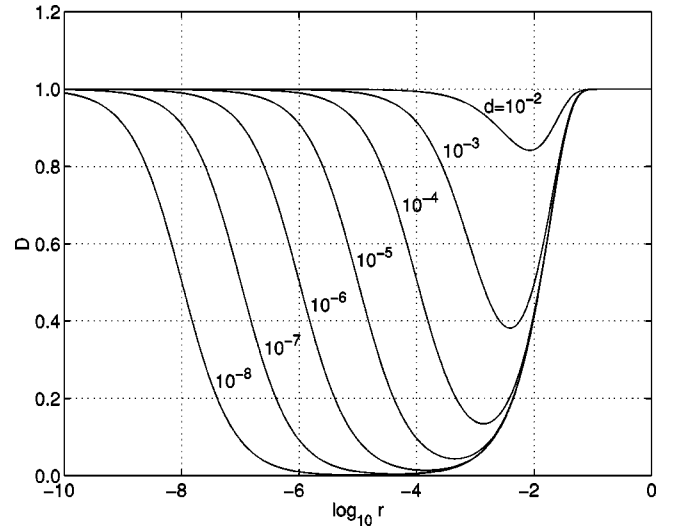
distance between the cutoffs is larger than 3 decades. Otherwise, an apparent fractal dimension extending over a range up to 2 decades appears, with an apparent d value changing progressively from zero to 1 as the density increases.

We analyzed several sets of points with normally distributed distances of fixed mean value Δ and different values of the standard deviation σ, ranging from zero (equispaced points) to Δ (see Figs. 3 and 4). The width of the corner region clearly increases with the dispersion of the interpoint distances, converging to the shape of the Poisson random distribution when $\sigma = \Delta$. We conclude that a width of 2 decades around the average distance cutoff is typical for objects distributed with a strong random component.

The shape of the transition around the lower cutoff is due to the redundancy of the box counting covering. As one can

FIG. 2. Local box counting dimension $D(r)$ for the same sets as in Fig. 1.
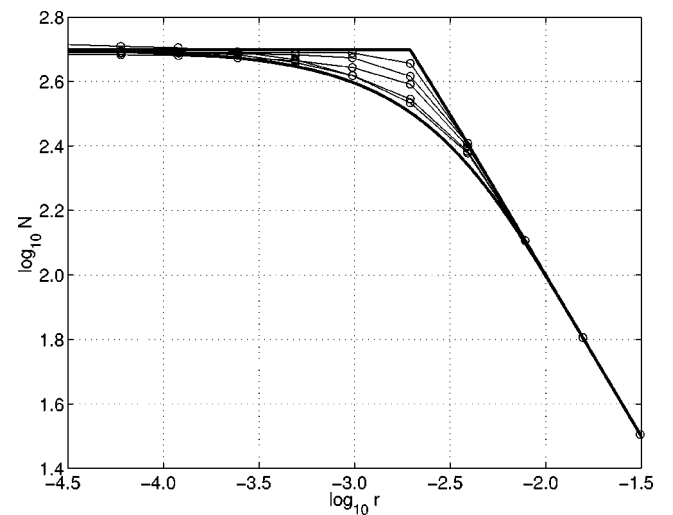

FIG. 3. Box counting $N(r)$ function for a set of 500 points with Gaussian interpoint distribution. Circled points correspond to a progressively increasing standard deviation $\sigma/\Delta = 0.2, 0.4, 0.6, 0.8, 1$. The two thick curves correspond to equispaced and random placed points (Poisson).
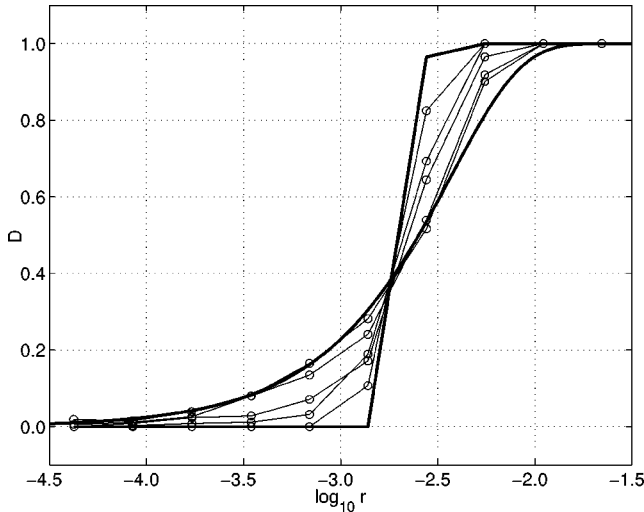
FIG. 4. Local box counting dimension $D(r)$ for the same sets as in Fig. 3.

observe in Fig. 5 the cutoff has substantially the same shape for a random set of 100 boxes of diameter $d=10^{-4}$ and for the same boxes distributed in an equispaced set. Analysis of the random set with the Bouligand minimal covering algorithm leads to a sharp cutoff (see Fig. 5). The redundancy of the BC covering depends on the random match between the uniform partition and the set points, but it is easy to show this to be statistically identical to that of the MS covering, which is simple to evaluate. The MS covered length for N_r separated rods of diameter d is

$$L(r)=N_r(d+r).\tag{3.1}$$

Dividing this expression by the diameter r of the MS balls, one obtains the equivalent number of boxes to be compared with the BC curves in Fig. 5. It is immediate to see that the concavity of the cutoff has, again, a typical width of a couple of decades, which is simply due to the presence of an additive constant to the power law due to the change of scaling.
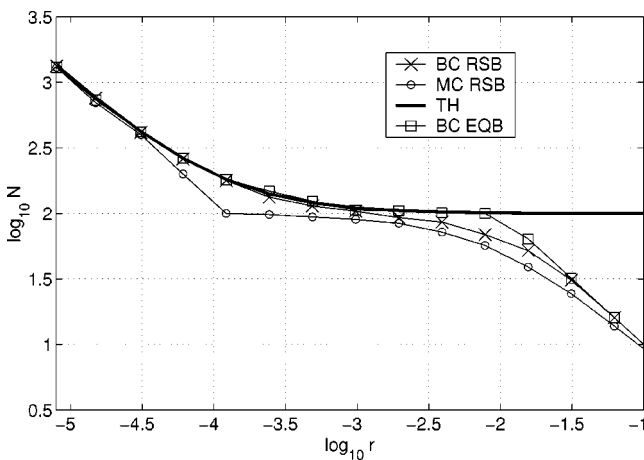

FIG. 5. Box counting (BC) and minimal covering (MC) $N(r)$ functions for 100 random (RSB) or equispaced (EQB) rods of length $\delta=10^{-4}$. The solid line represents the theoretical prediction of average redundancy.
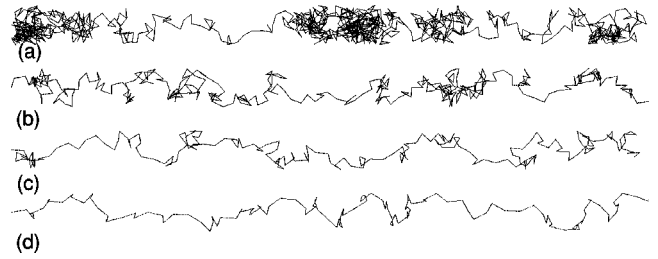

FIG. 6. Random walk drifted on a 2048×128 pixel stripe with velocities (a) $v=2$ pix/step, (b) $v=6$ pix/step, (c) $v=10$ pix/step, (d) $v=20$ pix/step.

B. Walker's ruler dimension

Apparent fractality can also be shown to emerge as an artifact of cutoffs with the Walker's ruler (WR) dimension by analyzing a drifted random walk of given step d. The particle is forced to move in a narrow strip of width w and drifted along the strip with a constant velocity v. Images of the resulting trace for several values of v are shown in Fig. 6 and their WR analysis is shown in Fig. 7. The set behaves as a line for rulers either shorter than the step d or longer than the width w of the strip. The slope in the intermediate region takes the typical random walk value of 2 for slow drift velocity, but it takes apparent fractal values progressively decreasing from 2 to 1 as the drift velocity is increased with consequent disentanglement. This nonuniversal apparent fractal scaling spans again approximately one or two decades. BC analysis of the same pictures yields very similar results and provides an apparent counterproof to the artifact.

C. The correlation dimension

The *correlation dimension* D_2 is estimated [5] as the slope of the log-log plot of $C(r)$,

$$C(r)=\lim_{N\to\infty}\frac{1}{N^2}\{\text{number of pairs } (i,j) \text{ with } |X_i-X_j|<r\}$$
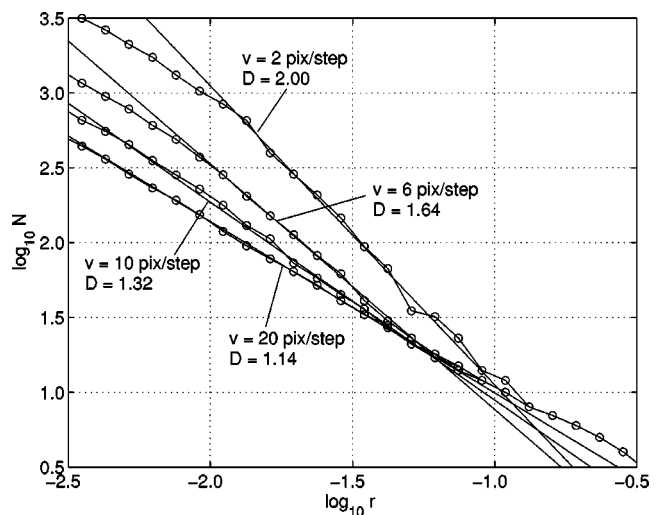
$$\sim r^{D_2}.\tag{3.2}$$

FIG. 7. Walker's ruler analysis of the curves of Fig. 6, along with the least squares fit of the linear regions.

Again, the presence of physical cutoffs in the data gives rise to smooth changes of scaling with the eventual emergence of apparent fractality. Kitoh *et al.* [6] showed that the cutoffs induce a concavity in their neighborhood due to the appearance of the additive constants to the power laws. This effect is identical to the one described in the BC section.

Several alternative estimators for the correlation dimensions were derived by Takens [7] and by Smith [8], mainly based on maximum likelihood. These statistical estimators are gathered by estimators of their variance, but they may prove to be inconsistent if physical cutoffs affect the scaling. Pisarenko *et al.* [9] proposed a method to estimate the presence of an upper cutoff in the power law, but the problem becomes very tricky if two cutoffs are present.

IV. A STRATEGY OF DEFENSE AGAINST THE PERNICIOUS EFFECT OF PHYSICAL CUTOFFS

Since a modest difference between the values of cutoffs is typical, the emergence of an apparent fractal scaling extending over up to a couple of decades is expected to be a very common feature, which is independent of an effective fractal nature of the sets. This is valid for both connected and unconnected images and is irrespective of the definition of fractal dimension. As a consequence, serious doubts emerge on all empirical fractal claims—the vast majority in practice [10]—which do not span more than two decades.

The presence and the nature of the physical cutoffs is not generally known *a priori* for a given empirical image, but experience may provide great help. In an image constituted of spots, one should estimate the average diameter of the spots and the average distance among them. For line-based images, such as river patterns and fracture network, the minimal length free of intersections or sharp corners represents a lower cutoff, and one should observe whether there is some scale at which the set appears to uniformly cover the embedding space. If one identifies the nature and the value of the cutoffs, one can guess what the scaling curve will look like, and, if the difference between these cutoffs is insufficient, one can conclude that it is useless to estimate the fractal dimension since it would be both inaccurate and meaningless.

While this may require great care in future issues, as well as reassessment of published ones, a quick-and-dirty thumb rule caution against the effect of physical cutoffs is to ensure that each fractal estimate spans over at least three decades.

[1] K. Falconer, *Fractal Geometry* (Wiley, New York, 1990), Chap. 1.

[2] G. Gonzato, F. Mulargia, and W. Marzocchi, Geophys. J. Int. **132**, 275 (1998).

[3] G. Gonzato, F. Mulargia, and M. Ciccotti, Geophys. J. Int. **142**, 108 (2000).

[4] D. Hamburger, O. Biham, and D. Avnir, Phys. Rev. E **53**, 3342 (1996).

[5] P. Grassberger and I. Procaccia, Phys. Rev. Lett. **50**, 346 (1983).

[6] S. Kitoh, M. Kimura, K. Mori, K. Takezawa and S. Endo, Physica D **141**, 171 (2000).

[7] F. Takens, Lect. Notes Math. **1125**, 99 (1984).

[8] R.L. Smith, *Nonlinear Modeling and Forecasting. SFI Studies in the Sciences of Complexity*, edited by M. Casdagli and S. Eubank (Addison-Wesley, Reading, MA, 1992), Proc. Vol. XII.

[9] D.V. Pisarenko and V.F. Pisarenko, Phys. Lett. A **197**, 31 (1995).

[10] O. Malcai, D.A. Lidar, O. Biham and D. Avnir, Phys. Rev. E **56**, 2817 (1997).